

1 **Developing a Methodology to Estimate the Retroreflectivity of Longitudinal**
2 **Pavement Markings using LiDAR**

3
4 **Abbas Mohammadi**

5 Department of Civil and Environmental Engineering
6 University of Utah, Salt Lake City, Utah, 84112
7 Email: Abbas.Mohammadi@utah.edu

8
9 **Juan C. Medina**

10 Department of Civil and Environmental Engineering
11 University of Utah, Salt Lake City, Utah, 84112
12 Email: Juan.C.Medina@utah.edu

13
14 **Abbas Rashidi**

15 Department of Civil and Environmental Engineering
16 University of Utah, Salt Lake City, Utah, 84112
17 Email: Abbas.Rashidi@utah.edu

18
19 **ABSTRACT**

20 Longitudinal pavement markings significantly affect traffic safety, particularly in adverse weather and
21 nighttime conditions when crashes and fatalities are often overrepresented. Given the wide range of
22 factors affecting the performance of pavement markings, periodic monitoring is needed to ensure their
23 integrity and adequate retroreflectivity levels. Typical monitoring methods include individual readings
24 from manual retroreflectometers and, more recently, mobile setups where much larger segments can be
25 covered in shorter periods. However, mobile setups require specialized equipment, calibration, and
26 significant economic resources. This research uses LiDAR data collected as part of asset management
27 efforts to help assess pavement marking retroreflectivity, reducing reliance on special-purpose equipment,
28 mainly for maintenance-related decisions. Identifying and isolating the pavement marking from the
29 LiDAR point cloud, filtering, and modeling are part of a proposed exploratory process to evaluate the
30 associations between field-measured retroreflectivity and a combination of intensity from LiDAR
31 readings, RGB data, and marking material. Freeway data covering over 300 miles of markings along
32 freeways are used to analyze the initial potential of LiDAR in assessing the retroreflectivity of pavement
33 markings. Results are encouraging and show that LiDAR data can produce reasonable associations to
34 retroreflectivity levels. However, significant questions remain open in terms of the transferability of
35 results, modeling other variables such as weather and traffic exposure, and the inherent differences that
36 may arise when evaluating different treatment materials and markings at different points within the
37 roadway (i.e., at varying distances and angles from the LiDAR sensor).

38
39 **Keywords:** Retroreflectivity pavement marking, LiDAR intensity, road marking management and
40 maintenance.

1 **INTRODUCTION**

2 Longitudinal pavement markings are essential to manage traffic and promote safe and consistent
3 driving patterns. However, road markings can fade due to tire friction, adverse weather conditions,
4 damage from snow removal equipment, and simple exposure to the elements, complicating their visibility
5 for human drivers and self-driving vehicles.

6 The effectiveness of longitudinal pavement markings is primarily hinged on their maintenance,
7 especially during low-light conditions and poor weather (1, 2). However, with more than 8.8 million lane
8 miles in the U.S., consistent monitoring and upkeep represent significant human and economic resources
9 to public agencies. Moreover, research by the National Cooperative Highway Research Program
10 (NCHRP) revealed that about 30% of state agencies carry out evaluations of pavement markings yearly,
11 while the rest undertake these assessments biennially or even less frequently (3).

12 A critical measure in assessing the condition and effectiveness of longitudinal pavement markings
13 is their retroreflectivity, which can be defined as the ratio of luminance to illuminance, measured in
14 candelas per square meter per lux (4). Here, luminance quantifies light intensity within a specific area as
15 perceived from a particular angle, while illuminance refers to the amount of light falling onto a surface.

16 More specifically, for roadway marking assessments, ASTM standards provide guidelines to
17 measure retroreflectivity so that it models the light reflected from the marking back to the driver in a
18 design setting. Current devices used to measure retroreflectivity following ASTM standards include
19 handheld retroreflectometers, and mobile counterparts adapted to mimic the same geometry described by
20 the standards, providing comparable results and maintaining uniformity in reported data.

21 However, even though mobile retroreflectometers provide significant advantages in data
22 collection speed and efficiency, such setups still need significant economic resources and highly
23 specialized equipment with limited device coverage, requiring several passes to assess all the roadway
24 cross-section markings fully. For example, six passes are needed to assess the retroreflectivity of marking
25 a four-lane divided highway (1, 2, 5). Moreover, the Federal Highway Administration (FHWA) is
26 introducing new standards to establish baseline levels of reflectiveness that pavement markings must meet
27 (6). Consequently, public agencies, including Departments of Transportation (DOTs), urgently need to
28 implement a method for maintaining minimum levels of retroreflectivity for markings, with compliance
29 for such requirements expected to be in place by September 2026. (2, 5).

30 Therefore, there are opportunities to improve the assessment of pavement marking
31 retroreflectivity both in terms of reducing the reliance on specialized equipment and personnel, as well as
32 economic resources, with the added pressure to implement a management plan to meet new FHWA
33 requirements in a timely fashion.

34 On the other hand, recent strides in mobile data collection and artificial intelligence have made it
35 possible to use mobile Light Detection and Ranging (LiDAR) for the automated detection and cataloging
36 of road assets. With several DOTs actively gathering mobile LiDAR data, the point cloud produced from
37 such data collection is a rich and valuable resource for crafting detection algorithms beyond asset
38 management. Along this line, LiDAR may also have the potential to provide a proxy to assess
39 retroreflectivity, and it could evaluate multiple lanes with a single pass.

40 This study explores leveraging existing LiDAR data collected for asset management to lay the
41 groundwork for establishing a comprehensive management system to assess the retroreflectivity of
42 pavement markings. The body of work in this area is still very limited. Thus, this research seeks to
43 contribute with empirical evidence, data post-processing methods, extraction of pavement marking data
44 from LiDAR datasets, and preliminary models aimed at overcoming limitations of direct retroreflectivity
45 measurement methods, which are labor-intensive, require significant economic resources and can only
46 evaluate a small portion of road markings at any given time. In addition, work on this direction is also
47 very timely, as it is expected to help enable a process for public agencies and DOTs to support
48 compliance with new FHWA standards for pavement marking reflectivity.

LITERATURE REVIEW

Deadly motor-vehicle crashes are over-represented during nighttime. Despite only a quarter of all travel happening at night, nighttime crashes account for half of the traffic-related fatalities (7). Therefore, it is crucial to oversee, enhance, and upkeep the road infrastructure that supports safety during nighttime driving. Studies indicate that enhancing the retroreflectivity of road markings and signs improves how far drivers can see and perceive their surroundings at night (8, 9), promoting safer driving.

The Manual on Uniform Traffic Control Devices (MUTCD) points out that the clarity of road markings can be significantly diminished by snow, debris, and water near these markings. The factors that affect how well road markings are seen are quite extensive and include infrastructure condition, pavement marking locations, placement quality, usage, material, color, contrast, design, condition, configuration, width, pattern, raised pavement markers, retroreflectivity, and local snow removal practices (10).

In addition to difficulties estimating the factors affecting pavement-making effectiveness, measuring the marking performance is also challenging, including quantifying their retroreflectivity. This review of relevant literature explores the topics of road markings, retroreflectivity, and, more importantly, the use of mobile LiDAR technology to assess the condition of pavement markings.

Materials for road markings are chosen depending on expected road conditions and budget constraints, among other considerations. Commonly utilized materials include paints, thermoplastics, and tapes, where the materials selected need to maintain their planned color over their lifespan and ensure that the markings do not decrease vehicle traction on the road, per MUTCD recommendations (7).

The deterioration of the retroreflectivity of road markings over time is perhaps the most critical factor in their performance, and it is influenced by several characteristics such as traffic flow, maintenance activities, climatic conditions, orientation, and precipitation. Within the first year of service life, some pavement markings experience a decline in their initial retroreflectivity by 33-40% (4), so conducting assessments of these installations is essential to gauge the marking effectiveness. Such evaluations help identify when the retroreflective materials are nearing the end of their utility, providing valuable information to improve cost efficiency and sustainable service. Techniques for these assessments include manual inspections during the night and retroreflectometers, as mentioned above, with the latter being the prevalent method for examining these assets (4, 11).

As an alternative technology to assess retroreflectivity in this paper, LiDAR technology operates by projecting laser beams and capturing the reflected light with a sensor to measure distances. The precise positioning of LiDAR devices enables the generation of three-dimensional representations that are accurately mapped to real-world locations. LiDAR is utilized across various domains, including land surveying, asset management, and remote sensing, and the scope of data acquisition can range significantly based on the sensors utilized and the collection technique employed, from aerial surveys covering entire communities to detailed examinations of pavement cracks. The efficiency of LiDAR allows for the rapid collection of data, significantly reducing the time required compared to traditional manual survey methods (12).

Besides capturing geometric information, LiDAR also records the intensity of laser light that bounces back to its sensor. This intensity data yields insights into the reflectivity of objects within the surveyed area and potentially a relative estimate of the retroreflectivity of pavement markings. However, a series of calibrations and processing steps must be undertaken to evaluate object reflectivity accurately using these intensity measurements (13).

Guan et al. (14) studied various methods for extracting road markings. They found that while many approaches are based on the geometric features of roads, some methods enhance accuracy by integrating additional data sources such as videos, maps, and aerial surveys to confirm the boundaries of the pavement.

The results of this data collection process are typically projected onto a two-dimensional plane for analysis, applying detection thresholds to specify road markings (15). Due to the projection, the accuracy can be affected by the varying distances between the sensor and the specific pavement marking being analyzed. To address this issue, researchers have adjusted the intensity values, considering both the distance and the angles to these more distant data points (16). Instead of modifying the recorded intensity

1 values, some researchers have decided to use the threshold for detection, making them variable based on
2 distances and angles (17).

3 Hou et al. (18) demonstrated using mobile LiDAR to locate and assess pavement markings by
4 developing and evaluating new automated LiDAR processing algorithms. Additionally, their research
5 investigated the feasibility of identifying the deterioration trend of retroreflectivity conditions. The study
6 involved developing a comprehensive pavement marking inventory with retroreflectivity conditions for
7 14 selected testing sections and comparing historical and current data to determine deterioration trends for
8 three marking materials: polyurea, epoxy, and thermoplastic.

9 Manasreh et al. (19) focused on predicting retroreflectivity using the intensity of mobile LiDAR
10 data, highlighting their correlation. The study provided a framework for pavement marking assessments
11 using relatively inexpensive LiDAR sensors, showcasing the potential of machine learning techniques in
12 this domain. The methodology included comprehensive feature extraction from LiDAR data, feature
13 selection, and evaluation of various learning algorithms, achieving an R-squared of 0.824 on unseen data.

14 Lastly, He et al. (20) introduced a vehicle-mounted LiDAR-based perception and evaluation
15 method for retroreflection of road traffic markings, aiming to address the inefficiency in retroreflection
16 maintenance. A calibration prediction model for LiDAR is established using a regression decision tree,
17 enabling accurate prediction of road markings' retroreflected luminance (RL) values. A maintenance
18 evaluation model was developed based on China's national standard, achieving an agreement of over 85%
19 with traditional methods and reducing time costs by at least 90%. The study compared multiple linear
20 regression functions, second-order polynomial functions, and decision trees for the calibration prediction
21 model, with the decision tree showing the best fit (coefficient of determination = 0.95).

22 In summary, despite few studies exploring the relationships between retroreflectivity of pavement
23 markings and LiDAR data, there are still significant open questions on several fronts, including the
24 selection and filtering of data from the LiDAR point cloud, models to best represent such relationships,
25 the effects of treatment materials, external conditions, elapsed in-service time, and angle and distance of
26 the intensity reading, among others. The following sections propose ideas and discuss outcomes on some
27 of the open questions, identifying promising methods, outcomes, and further work to continue moving
28 towards a lower reliance on specialized data and equipment for assessing the retroreflectivity of pavement
29 markings.

30 31 **DATA DESCRIPTION AND PROCESSING**

32 This study used two primary data sources to analyze potential associations between field-
33 measured retroreflectivity and LiDAR outcomes, as described below.

- 34
- 35 - **Retroreflectivity Data:** The dataset contains detailed retroreflectivity measurements collected in
36 the field from a mobile setup calibrated to represent data collection methods for pavement
37 markings following ASTM standards. Each row in this dataset represents a distinct location along
38 the highway, identified by the section milepost, the average retroreflectivity, and counts of both
39 valid and invalid measurements, offering insights into the data's reliability. Field measurements
40 are typically presented every 0.1 miles.
 - 41
 - 42 - **LiDAR Data:** The LiDAR data was received from a vendor that surveys state-managed routes for
43 the Utah DOT (UDOT), and it was provided in .las or .laz formats, which are standard for LiDAR
44 data but complex to work with directly. To make this data more manageable, it was converted
45 into a CSV (Comma-Separated Values) format using Python. This step is crucial as it integrates
46 LiDAR data with other datasets, enabling comprehensive analysis and correlation with
47 retroreflectivity data. The processed LiDAR data includes X, Y, and Z coordinates, which
48 provide the 3D spatial locations of points on the highway. Additionally, the data contains
49 intensity values, indicating the strength of the laser beam return, and RGB values, which help
50 visualize the data closer to how it appears.
- 51

1 It is noted that the coordinate system used in the LiDAR data (UTM Zone 12 N) differs from the
2 retroreflectivity data (WGS 84). Therefore, a conversion process aligned these datasets for effective
3 comparison using appropriate scale and offset values in the LiDAR data information. After conversion,
4 the dataset included new columns for latitude and longitude, allowing direct comparison and integration
5 with the retroreflectivity data.
6

7 **Post-Processing LiDAR and Retroreflectivity Datasets**

8 The post-processing phase involved extracting lane marking information from the LiDAR datasets and
9 integrating it with retroreflectivity measurements. This process is critical for ensuring the accuracy and
10 reliability of the data analysis. The steps in this process are described next and illustrated in Figure 1.
11

- 12 a) Location of Markings within LiDAR Cross-Section: The first step involved identifying lane
13 markings within the LiDAR data cross-section using the field retroreflectivity measurements. We
14 created a rectangular sampling area centered on the point representing the field retroreflectivity
15 reading to do this. This rectangle is large enough (i.e., 30 ft by 15 ft) to include all relevant data
16 around the corresponding lane marking (Figure 1(a)).
- 17 b) Filtering Using Intensity Values: Once the lane markings are located, they are filtered based on
18 their intensity values. A grid of points spaced 0.2 feet apart inside the rectangular sampling area is
19 created (see Figure 1(b)). This detailed grid allows for a precise cross-section of the LiDAR data
20 at the exact location of the lane marking, facilitating more accurate analysis.
- 21 c) Identification of Next Sampling Area: After processing one area, the next sampling area is
22 identified using the previous sampling area as a reference, as shown in Figure 1(c). This ensures
23 that the new area aligns with the actual direction of the road lines confirmed in the previous
24 iteration.
- 25 d) Continuous Presence Verification: The fourth step involves verifying the continuous presence of
26 lane markings within the sampling area. If lane markings are consistently present, the process
27 moves to the next area and repeats the filtering in step (b). If not, the process skips to the location
28 of the subsequent retroreflectivity measurement described in step (a).
29

30 This iterative process effectively ensured data accuracy and minimized errors in identifying lane
31 markings.
32
33
34
35
36
37
38
39
40

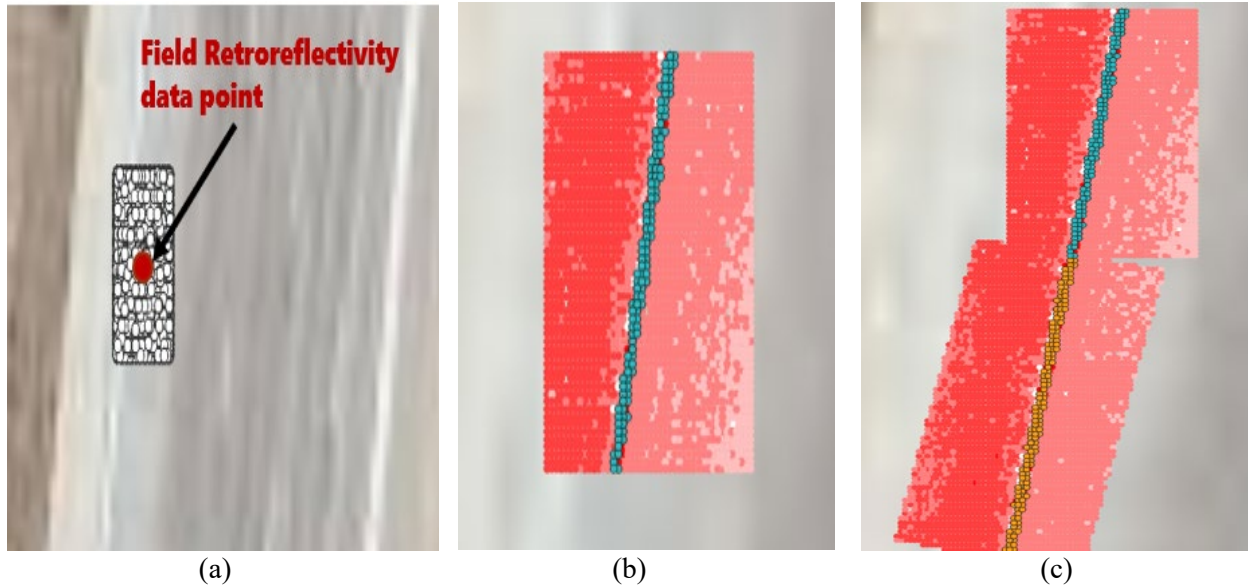


Figure 1 Illustration of Postprocessing LiDAR Data: a) Location of Markings within LiDAR Cross-Section, b) Filtering Using Intensity Values, and c) Identification of Next Sampling Area

The filtering stage described above as step (b) is a critical step that deserves additional discussion. For the filtering to be effective, this research took into consideration the following observations:

- The RANSAC (Random Sample Consensus) algorithm was applied to the selected area to filter out noise and irrelevant data points. This technique focused on points likely to represent road markings, improving the accuracy of our analysis.
- Within the sampling area, each dot in the LiDAR data represents a measurement, with its color indicating the intensity or brightness of the return. So, the process identified points with high relative intensity within the search area, as these are likely to belong to the pavement marking subject to evaluation.
- After identifying points likely to represent the pavement marking and filtering out less relevant points, the remaining high-intensity points form a line identified as road marking. Figure 1(b) shows the blue dots composed of these high-intensity points, confirming the presence of a road marking. This line is added to our dataset of confirmed road markings, allowing us to build sets of layers with each pavement marking to be assessed.

An illustration of the overall method in schematic form is shown in Figure 2.

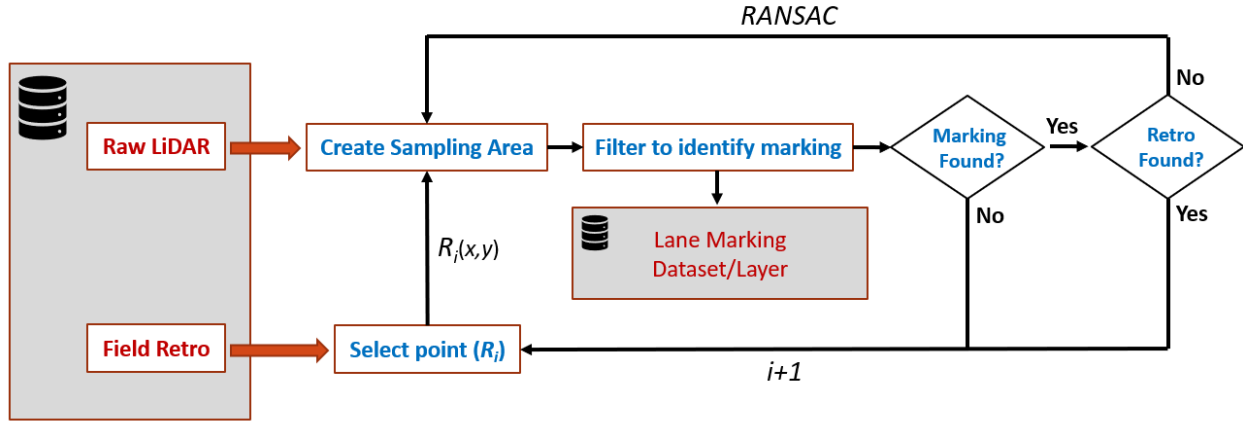


Figure 2 Schematic illustration of data post-processing method

RESULTS AND MODELING

This section presents the outcomes of an evaluation using the methods described above, including sections of interstates I-15 and I-84 in Utah, where the right and left continuous edge lines were extracted.

The mileposts and total number of points included from each of the interstates and travel directions along the continuous edge line are shown in Table 1. It is noted that during the preprocessing phase, some data points were disregarded due to low-quality observations in the field retroreflectivity readings or due to the presence of highway ramps. Each data point includes detailed information such as retroreflectivity, average LiDAR intensity, latitude, longitude, material type, and average RGB values.

Table 1. Summary of Sample Data Extracted

Pavement Marking	Route	Direction	Total miles	Total Points
Right edge line	I-15	Northbound	86	363
		Southbound	89	321
	I-84	Eastbound	32	191
		Westbound	37	205
Left edge line	I-84	Eastbound	32	204
		Westbound	37	216

The first results section is focused on readings along the continuous right edge line, while the second section illustrates results from the left edge line.

Right Edge Line Data

Scatter plots of the field-measured retroreflectivity Vs. the average LiDAR intensity for the right edge line cases are shown in Figure 3 and Figure 4. The scatter plots generally indicate a positive correlation between LiDAR average intensity values and field-measured retroreflectivity, as expected, where the rate of increase of retroreflectivity in terms of LiDAR intensity is also gradually increasing, suggesting the potential for non-linear relationships. In addition, different clusters are visible in the plots, sometimes representing groups of data points from sections with the same treatment material but also indicating the presence of segments with different in-service times (i.e., different treatment installation dates).

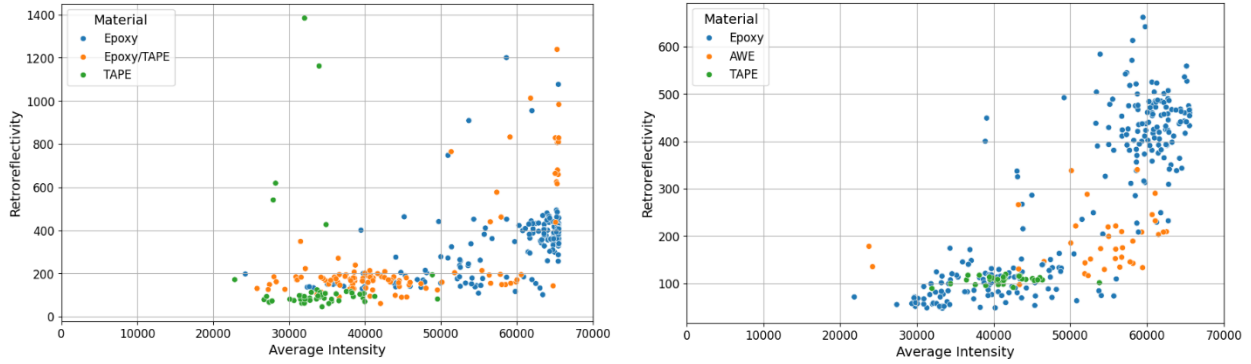


Figure 3. I-15 Right edge line retroreflectivity and intensity: a) Northbound and b) Southbound

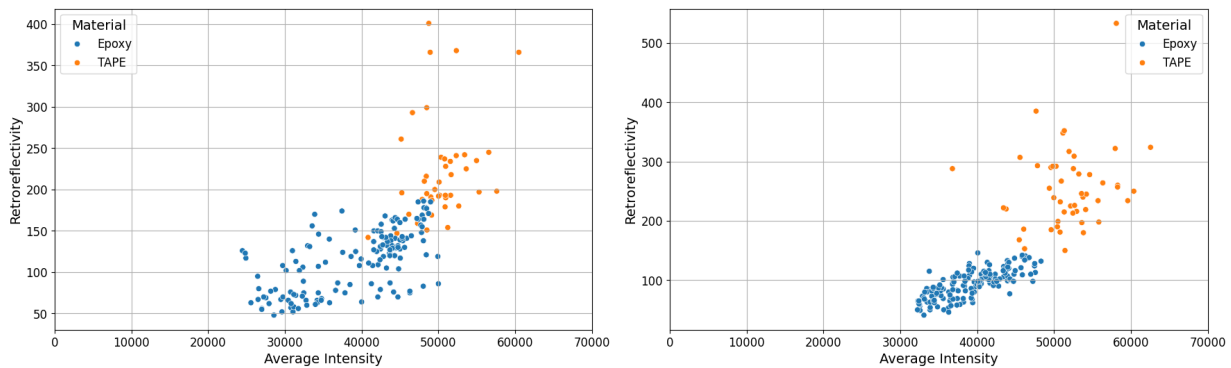


Figure 4. I-84 Right edge line retroreflectivity and intensity: a) Eastbound and b) Westbound

Before the modeling exploration, steps to conduct outlier removal and normalization were conducted to prepare the datasets. Outliers were analyzed using the Modified Z-Score method, where the median and median absolute deviation (MAD) between retroreflectivity and LiDAR intensity identified were used to identify outliers outside a Modified Z-score range between -3.5 and 3.5. Lastly, intensity values were normalized using Min-Max Scaling to bring the average LiDAR intensity values into a range between 0 and 1.

Two regression models, including an exponential model and an XGBoost model, were developed to establish associations between the field-measured retroreflectivity and up to three independent variables (i.e., LiDAR intensity, average LiDAR Red value from the RGB data, and material type). The functional form of the exponential model was chosen given initial observations from the scatter plots and is shown in Equation 1 below:

$$Y = a * (e^{(b+cX)}) \tag{Eq. 1}$$

Where,

- Y = Field measure retroreflectivity
- X = vector of independent variables
- a,b,c = model constants

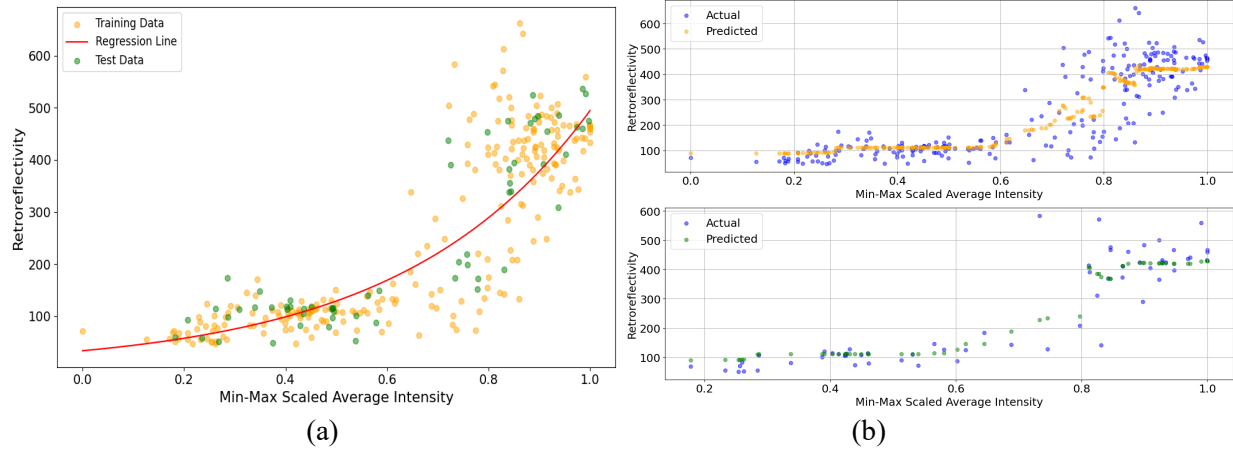
The overall modeling results are summarized in **Table 2** with key metrics such as RMSE and R². In addition, an illustration of the models for each case is shown in Figures 5 through 8.

1
2
3

Table 2 Right Edge Line Models - Performance Metrics Summary

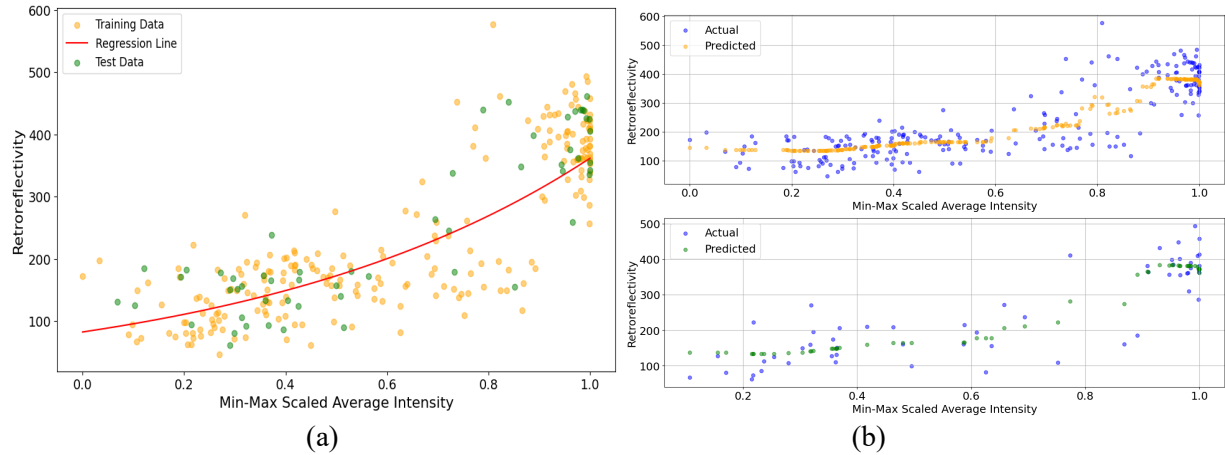
Road Marking	RMSE		R ²	
	Exponential	XGBoost	Exponential	XGBoost
1-15 REL NB	67	61	0.71	0.76
I-15 REL SB	85	74	0.75	0.81
I-84 REL EB	25	25	0.74	0.74
1-84 REL WB	28	25	0.81	0.85

4



5
6
7
8
9

Figure 5 I-15 southbound right edge line models: a) exponential model and b) XGBoost model



10
11
12
13
14

Figure 6 I-15 northbound right edge line models: a) exponential model and b) XGBoost model

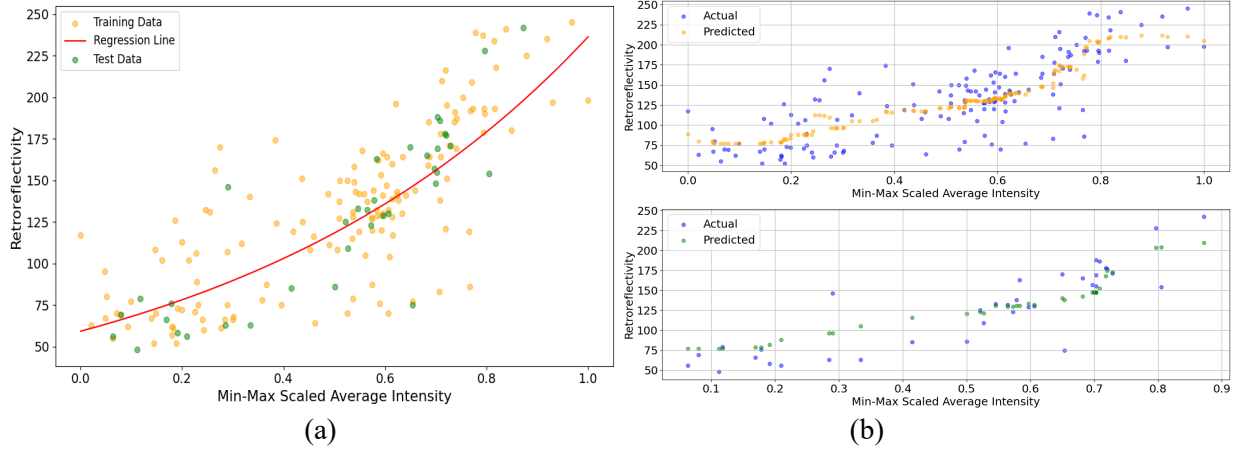


Figure 7 I-84 eastbound right edge line models: a) exponential model and b) XGBoost model

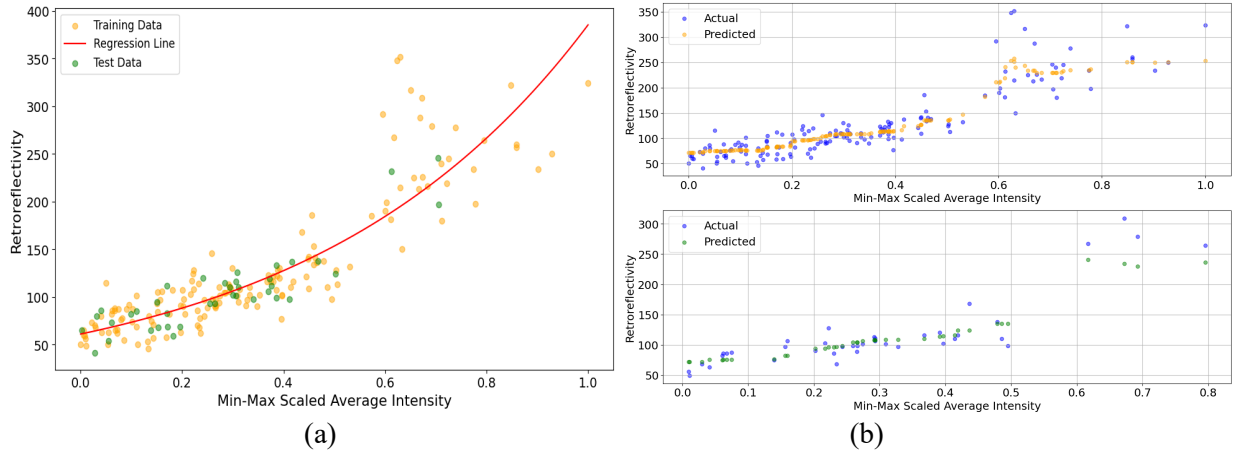
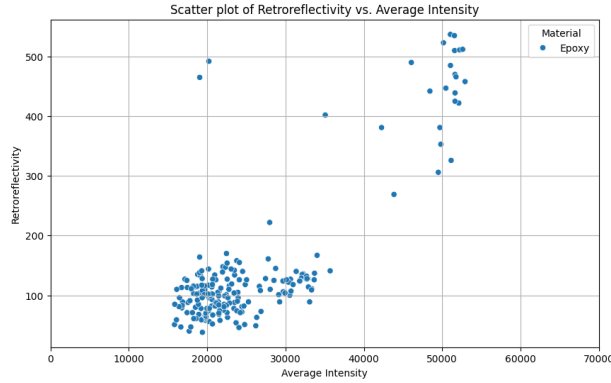


Figure 8 I-84 westbound right edge line models: a) exponential model and b) XGBoost model

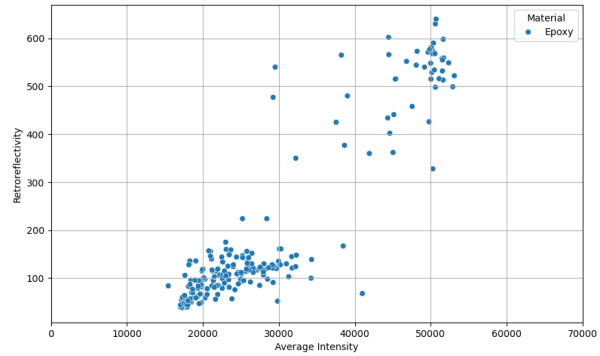
Left Edge Line Data

As mentioned above, data from the left edge line was also analyzed for similar sections of I-84. Part of the reasoning for reviewing the trends from the markings of a different lane was to identify potential deviations in the relationships observed above between retroreflectivity and LiDAR intensity, given that the LiDAR measurements would be taken from a location at a different angle and distance from the sensor. As reported in previous research, this could result in different reading patterns and, therefore, a potentially different modeling outcome.

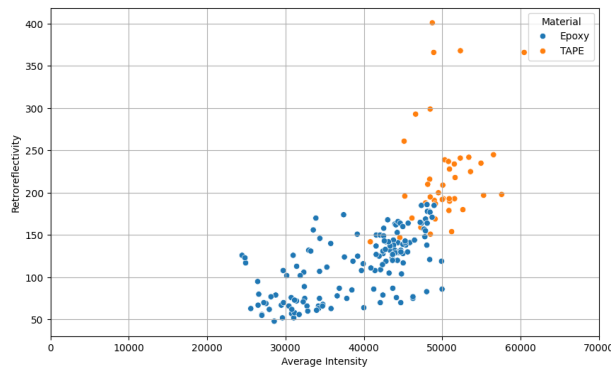
The scatter plots for the right and left edge lines in the two directions of travel on I-84 are shown in Figure 9 to initiate such discussion.



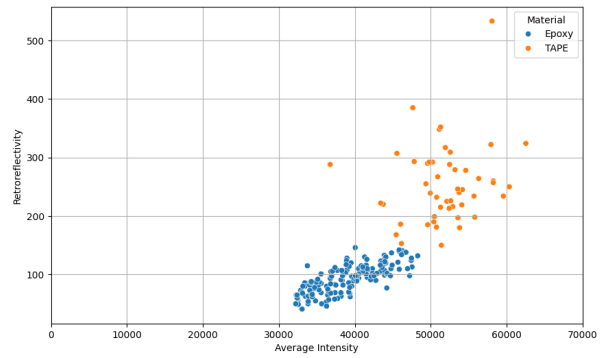
a) Left edge line Eastbound



b) Left edge line Westbound



c) Right edge line Eastbound



d) Right edge line Westbound

Figure 9 I-84 Right and left edge line data for eastbound and westbound directions

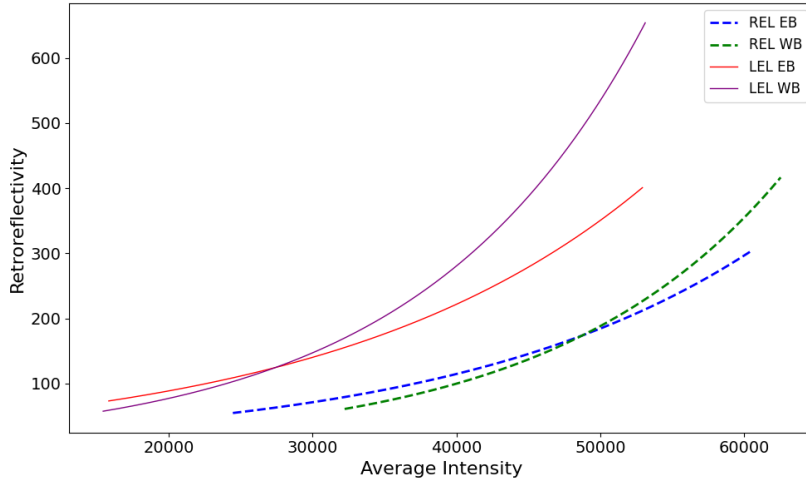
From Figure 9, a shift seems to exist towards lower LiDAR intensities for similar values of retroreflectivity, so, for example, retroreflectivity values below 200 mc/l/m² on the right edge line can be associated with LiDAR intensities of about 25,000 to 50,000 units in the original LiDAR dataset. However, the same retroreflectivity level on the left edge line corresponds to intensity values between 15,000 and 40,000 units.

The results from the left edge line models are shown in Table 3, where the model metrics provide similar outcomes and fitness indications as those for the right edge lines, with perhaps an improved fit to both models, particularly in terms of R².

Table 3 Left Edge Line Models - Performance Metrics Summary

Road Marking	RMSE		R ²	
	Exponential	XGBoost	Exponential	XGBoost
I-84 LEL EB	30	41	0.91	0.85
I-84 LEL WB	45	35	0.94	0.96

1 However, the suspected shift between intensities from the left to the right edge lines is more
 2 evident when the model outcomes are visualized together, as shown in Figure 10. From the figure, similar
 3 levels of field-measured retroreflectivity are expected at different levels of LiDAR intensity, with lower
 4 intensities for the left-edge line. Potential explanations for this shift are likely to relate to a combination of
 5 two factors: 1) the distance and angle from the LiDAR sensor to the measured marking, with the right
 6 edge line being at a closer distance and a higher (more perpendicular) angle, and the color difference,
 7 with the right edge line being white versus the left edge line having a yellow color.
 8



9
 10 **Figure 10 I-84 Right and left edge line exponential models**

11
 12 **DISCUSSION**

13 The results of this study highlight the feasibility of using LiDAR data to estimate the
 14 retroreflectivity of longitudinal pavement markings, offering a cost-effective and efficient alternative to
 15 traditional methods. This section compares the findings with previous research, highlighting key
 16 similarities and differences in functional forms, accuracy, and data utilization.

17 In line with the study by Hou et al. (18), our research also utilized mobile LiDAR data to locate
 18 and assess pavement markings. However, while Hou et al. focused on 14 selected testing sections with
 19 specific materials like polyurea, epoxy, and thermoplastic, our study covered a more extensive dataset,
 20 including over 300 miles of markings along two interstate highways. This broader scope allowed us to
 21 explore various pavement conditions and materials, providing additional insights on modeling outcomes
 22 from extensive in-service roadway data.

23 The functional forms used in our modeling—specifically the exponential and XGBoost models—
 24 demonstrated a strong fit, with R^2 values ranging from 0.71 to 0.96. This aligns with the findings of
 25 Manasreh et al. (19), who achieved an R^2 of 0.824 using machine learning techniques to predict
 26 retroreflectivity from LiDAR intensity data. However, our study's multiple regression models, including
 27 the more sophisticated XGBoost model, allowed for a more nuanced analysis of the relationships between
 28 LiDAR data and retroreflectivity, accommodating non-linear relationships and providing higher accuracy
 29 in some instances. Our study's choice of functional forms was guided by initial observations from scatter
 30 plots, suggesting non-linear relationships between LiDAR intensity and retroreflectivity. The exponential
 31 model, capturing the rate of increase in retroreflectivity with increasing LiDAR intensity, provided a
 32 reasonable approximation for most data points. However, the XGBoost model, with its capacity to handle
 33 complex interactions and non-linearities, outperformed the exponential model in several scenarios, mainly
 34 when accounting for additional variables such as material type and RGB values.

35 Our accuracy assessment showed that both models performed well, but the XGBoost model
 36 consistently provided better performance metrics, as evidenced by lower RMSE values and higher R^2
 37 scores. For example, in the I-15 southbound right edge line data, the XGBoost model achieved an R^2 of

1 0.81 compared to 0.75 for the exponential model, indicating a more accurate representation of the
2 observed retroreflectivity levels.

3 Our dataset was significantly more extensive than the Ai and Hennessy study (2), which also
4 employed mobile LiDAR for pavement marking assessments. Ai and Hennessy's research focused on a
5 specific region with a limited dataset, whereas our study spanned multiple highways and included a
6 diverse range of marking conditions. Additionally, the granularity of our data collection, with field
7 retroreflectivity measurements taken every 0.1 miles and corresponding LiDAR data processed to include
8 intensity, RGB values, and 3D spatial coordinates, provided a rich dataset for analysis. This level of detail
9 enabled us to develop more accurate models and offered valuable insights into the variation of
10 retroreflectivity across different pavement marking materials and conditions.

11 The findings of this study align with previous research in demonstrating the potential of LiDAR
12 data for assessing pavement marking retroreflectivity. However, our broader data coverage, sophisticated
13 modeling approaches, and detailed data processing set this study apart by providing new and valuable
14 insights and a more comprehensive understanding of the potential of LiDAR technology in this
15 application.

16 The success of the XGBoost model, in particular, suggests that advanced machine learning techniques
17 can significantly enhance the accuracy of retroreflectivity predictions from LiDAR data. These results
18 have important implications for public agencies and DOTs, offering a viable path toward more efficient
19 and cost-effective pavement marking assessments. As LiDAR technology continues to evolve and
20 become more accessible, the methodologies developed in this study could play a crucial role in meeting
21 new FHWA standards for pavement marking reflectivity, ultimately contributing to improved road safety
22 and maintenance practices.

24 **CONCLUSIONS AND FUTURE WORK**

25 This study presents empirical evidence, data post-processing methods, including extracting
26 pavement marking data from LiDAR datasets, and preliminary models to assess the retroreflectivity of
27 longitudinal pavement markings. The idea behind leveraging LiDAR data for this purpose stems from an
28 opportunity to reduce reliance on specialized magnetometer setups (including mobile setups) to provide
29 inputs to guide maintenance programs that guarantee adequate retroreflectivity levels. Such maintenance
30 programs are essential for traffic safety purposes and, more recently, are also required by FHWA to
31 demonstrate minimum in-service retroreflectivity levels.

32 The outcomes presented in this paper support the existence of specific associations between
33 retroreflectivity and LiDAR intensity that can be modeled with enough precision to support pavement
34 marking programs. Both an exponential model and XGBoost-based models can produce R^2 values
35 between 0.71 and over 0.90 depending on the travel direction and lane marking, and more importantly,
36 produce low RMSE values (between 25 and 85 mc/m²/l), suitable for overall evaluations (albeit through
37 additional data analysis) of retroreflectivity levels and determination of compliance with minimum
38 requirements.

39 However, significant additional work in this area is still needed to understand better the
40 implications of distance and angle of the marking to the LiDAR sensor, to mark material and color, and to
41 establish more reliable models to produce high-confidence assessments to support seasonal and yearly
42 maintenance decisions.

44 **ACKNOWLEDGMENTS**

45 This work was supported by the Utah Department of Transportation as part of contract No.
46 248331, with extended funding from the Center for Transformative Infrastructure Preservation and
47 Sustainability, University Transportation Center. Any opinions, findings, conclusions, or
48 recommendations expressed in this manuscript are those of the authors and do not necessarily reflect the
49 view of the funding agencies.

1 AUTHOR CONTRIBUTIONS

- 2 The authors confirm contribution to the paper as follows: study conception and design: A. Mohammadi,
3 J.C. Medina, A. Rashidi; data collection: A. Mohammadi; analysis and interpretation of results: A.
4 Mohammadi, J.C. Medina, A. Rashidi; draft manuscript preparation A. Mohammadi, J.C. Medina. All
5 authors reviewed the results and approved the final version of the manuscript.

REFERENCES

1. Mahlberg JA, Cheng Y-T, Bullock DM, Habib A. Leveraging LiDAR intensity to evaluate roadway pavement markings. *Future transportation*. 2021;1(3):720-36.
2. Ai C, Hennessy E. A pavement marking inventory and retroreflectivity condition assessment method using mobile LiDAR. Massachusetts. Dept. of Transportation. Office of Transportation Planning, 2022.
3. Hawkins NR. Use of transportation asset management principles in state highway agencies: Transportation Research Board; 2013.
4. Migletz J, Graham JL, Bauer KM, Harwood DW. Field surveys of pavement-marking retroreflectivity. *Transportation Research Record*. 1999;1657(1):71-8.
5. Zehr S, Hardin B, Lowther H, Plattner D, Wells T, Habib A, Bullock DM. Rumble Stripes and Pavement Marking Delineation. United States. Department of Transportation. *Intelligent Transportation ...*, 2019.
6. FederalRegister. National standards for traffic control devices; the manual on uniform traffic control devices for streets and highways; maintaining pavement marking retroreflectivity 2023. Available from: <https://www.federalregister.gov/documents/2022/08/05/2022-16781/national-standards-for-traffic-control-devices-the-manual-on-uniform-traffic-control-devices-for>.
7. (FHWA). Nighttime visibility - safety 2020. Available from: https://safety.fhwa.dot.gov/roadway_dept/night_visib/general-information.cfm.
8. Olsen MJ, Parrish C, Che E, Jung J, Greenwood J. Lidar for maintenance of pavement reflective markings and retroreflective signs. Oregon. Dept. of Transportation, 2018.
9. Pike A, Barrette T. Pavement Markings—Wet Retroreflectivity Standards. 2020.
10. Van Schalkwyk I. Enhancements to pavement marking testing procedures. Oregon. Dept. of Transportation. Research Section, 2010.
11. Kirk AR, Hunt EA, Brooks EW. Factors affecting sign retroreflectivity. Oregon. Dept. of Transportation, 2001.
12. Nolan J, Eckels R, Evers M, Singh R, Olsen M. Multi-pass approach for mobile terrestrial laser scanning. *ISPRS Annals of the Photogrammetry, Remote Sensing and Spatial Information Sciences*. 2015;2:105-12.
13. Kaasalainen S, Jaakkola A, Kaasalainen M, Krooks A, Kukko A. Analysis of incidence angle and distance effects on terrestrial laser scanner intensity: Search for correction methods. *Remote sensing*. 2011;3(10):2207-21.
14. Guan H, Li J, Cao S, Yu Y. Use of mobile LiDAR in road information inventory: A review. *International Journal of Image and Data Fusion*. 2016;7(3):219-42.
15. Yang B, Fang L, Li Q, Li J. Automated extraction of road markings from mobile LiDAR point clouds. *Photogrammetric Engineering & Remote Sensing*. 2012;78(4):331-8.
16. Zhang H, Li J, Cheng M, Wang C. Rapid inspection of pavement markings using mobile LiDAR point clouds. *The International Archives of the Photogrammetry, Remote Sensing and Spatial Information Sciences*. 2016;41:717-23.
17. Kumar P, McElhinney CP, Lewis P, McCarthy T. Automated road markings extraction from mobile laser scanning data. *International Journal of Applied Earth Observation and Geoinformation*. 2014;32:125-37.
18. Hou Q, Ai C, Boudreau N. An Automated Pavement Marking Retroreflectivity Condition Assessment Method Using Mobile LiDAR and Video Log Images. *Journal of Infrastructure Systems*. 2024;30(2):04024004.
19. Manasreh D, Nazzal MD, Abbas AR. Feature-centric approach for learning-based prediction of pavement marking retroreflectivity from mobile LiDAR data. *Buildings*. 2023;14(1):62.
20. He H, Xu A, Han X, Wang H, Wang L, Su W. LiDAR perception and evaluation method for road traffic marking retroreflection. *Transportation research record*. 2023;2677(6):258-79.

This paper was prepared for presentation at the 2025 Transportation Research Board (TRB) Annual Meeting.